VALORISATION OF RAPESEED AS BIOSORBENT FOR THE REMOVAL OF TEXTILE DYES FROM AQUEOUS EFFLUENTS

IRINA MOROSANU,[*] ANDREEA-FLORINA GILCA,[*] CARMEN PADURARU,[*]
DANIELA FIGHIR (ARSENE),[*] CATALINA ANISOARA PEPTU[**] and CARMEN TEODOSIU[**]

[*]*Department of Environmental Engineering and Management, Faculty of Chemical Engineering and Environmental Protection, "Gheorghe Asachi" Technical University of Iasi, 73 Prof. dr. D. Mangeron Str., 700050 Iasi, Romania*
[**]*Department of Natural and Synthetic Polymers, Faculty of Chemical Engineering and Environmental Protection, "Gheorghe Asachi" Technical University of Iasi, 73 Prof. dr. D. Mangeron Str., 700050 Iasi, Romania*
✉ *Corresponding author: C. Teodosiu, cteo@tuiasi.ro*

Lignocellulosic materials have been recognized as efficient, renewable and low-cost sorbents for the removal of dyes from effluents generated during textile processing. The objective of this work was to assess the suitability and efficiency of rapeseed biomass for the retention of Reactive Blue 19 dye from aqueous effluents. The effect of several variables on the sorption process in batch mode as a function of solution pH, initial dye concentration, contact time and temperature has been studied at laboratory scale. Removal efficiencies of over 49.63% were recorded for all experiments in the batch mode of operation. The experimental results show that the amount of dye retained onto rapeseed is proportional with the concentration and it has a faster rate of dye removal in the first 60 minutes. The kinetics of dye sorption has the highest correlation with the pseudo-second order model. Three widely used isotherm models (Langmuir, Freundlich and Dubinin-Raduskevich) were used to fit the experimental data. Thermodynamics analysis indicated the spontaneous and endothermic nature of the process.

Keywords: sorption, Reactive Blue 19, rapeseed, isotherms, wastewater

INTRODUCTION

Society progress is possible due to industrial development. On the other hand, industry, a large water consumer, has caused damage to the environment through the unsustainable use of natural resources and the generation of emissions into air and water, and of solid wastes. In recent years, the increased presence of synthetic dyes in effluents discharged from many industrial sectors, such as textile, leather, plastic, paper printing and food industries, into the environment has received great attention. Color-loaded wastewaters pose severe environmental problems, *i.e.* damage the aesthetics of water bodies, obstruct the penetration of light and oxygen transfer, present toxicity to aquatic biota.[1] Reactive dyes are intensely used in the textile industry. This type of dyes has high water solubility and can form covalent bonds between dye molecule and fiber.[2] However, about 12-15% of the dye remains unfixed, resulting in high concentration in the textile wastewaters.[3,4]

Reactive Blue 19 (Remazol Brilliant Blue R) is an anionic anthraquinone class dye used for dyeing and printing cellulosic fibers. Being a typical anthraquinone-based dye, the effluent containing RB19 is difficult to treat in environmental systems because of its polyaromatic structure (Fig. 1) and stability (half-time of RB-19 is 46 years at pH 7 and a temperature of 25 °C).[5] Moreover, it has a toxic and mutagenic effect on living organisms due to the presence of electrophilic vinylsulfone groups.[6] Therefore, the removal of this type of compound from different kinds of wastewaters presents great interest.

Various physical, chemical and biological treatment processes have been applied for the degradation/removal of the dye from wastewater.

They include membrane technology,[7,8] adsorption and biosoption,[9-11] biological processes,[12-14] advanced oxidation processes,[15-17] combined processes (ultrasound, photocatalytic, electrochemical, membrane, biological, *etc.*).[18-22]

These processes present advantages and disadvantages regarding their removal efficiency, costs and environmental impacts, and the selection of a preferred alternative is usually accomplished by means of multi-criteria analysis.

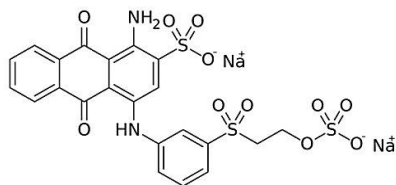

Figure 1: Chemical structure of Reactive Blue 19

Adsorption has proven to be an efficient method for treating dye wastewater.[3,11,23,24] Activated carbon is widely used in this process due to its high surface area and adsorption capacity, but it has the disadvantage of being expensive.[25] A sorbent should be accessible in large quantities, easy to regenerate and inexpensive.[26] From the point of view of green chemistry, biosorption with low-cost sorbents, such as natural materials, is closely related to the "use of renewable resources".[27] From the economic point of view, it was estimated that biosorption processes would reduce 20% of capital costs, 36% of operational costs and 28% of total treatment costs when compared with conventional systems.[28]

Many researchers have reported the feasibility of lignocellulosic materials in the sorption process.[10,29-31] This biomass predominantly derives from plants, trees and crops and such, containing lignin, cellulose, hemicellulose and other organic substances with many functional groups useful in adsorption of pollutants from aqueous media.[32] The potential of several natural materials has been investigated for dye minimization from aqueous effluents: tucuma cake,[33] canola hull,[34] deoiled soya,[1,35] rice straw,[36] tea waste,[30] orange bagasse,[25] garden pea,[27] pomelo peel,[37] citrus waste biomass,[38] sugarcane bagasse,[39] jackfruits seed flakes,[40] corn residues,[41,42] *etc.*

In the present study, rapeseed biomass was used for the removal of anionic dye Reactive Blue 19 (RB19) from aqueous solution. To the authors' knowledge, the potential of rapeseed to remove this type of dye from aqueous solutions was not previously evaluated. In this paper, investigations regarding the surface of the rapeseed and its capability as a sorbent were made, with a focus on

the operational parameters affecting the sorption process, *e.g.* pH, initial dye concentration and contact time. The experimental data were analyzed using the pseudo-first-order, pseudo-second-order, intra-particle diffusion and film diffusion kinetic models. The Langmuir, Freundlich and Dubinin-Raduskevich isotherm equations were applied to the experimental data. Thermodynamic parameters were also determined.

EXPERIMENTAL

Sorbent preparation and characterization

The rapeseed used as sorbent in this study was collected from agricultural units around Iasi, Romania. In order to remove dust and soluble pollutants, the biomass was first washed with deionized water several times and then dried at 40 °C for 24 h. The dried samples were milled (Retsch-Grindomix-GM-200) to obtain particle sizes of 0.1-0.2 mm.

The chemical and morphological characteristics of the rapeseed biomass were analyzed by infrared spectroscopy (IR) and scanning electron microscopy (SEM). Attenuated total reflection Fourier transform infrared spectroscopy (ATR-FTIR) measurements were performed on a Platinum ATR ALPHA (Bruker, Germany) spectrometer with a single reflection diamond ATR sampling module. All spectra were recorded with a resolution of 2 cm^{-1} in the range 400-4000 cm^{-1}, with 128 acquisition scans.

The morphology of the rapeseed samples before and after sorption was observed with a HITACHI SU 1510 optical microscope, operating at 20 kV.

Chemicals

Reactive Blue 19 dye was supplied by Bezema Co. (Switzerland), and used without further purification. A stock solution of 1 g L^{-1} was prepared by dissolution of 0.5 g RB19 and dilution to 500 mL. Working solutions were obtained by appropriate dilutions of the stock solution.

For the determination of the influence of medium acidity upon the process, a solution of 0.1 M H_2SO_4 or NaOH has been used, and the pH was determined by a WTW-340i pH-meter.

Sorption experiments

The characteristics of RB19 sorption onto rapeseed were determined by studying the effect of pH, initial dye concentration and contact time, sorption isotherms, sorption kinetics and sorption thermodynamics. The experiments were performed following the batch procedure. For all the measurements, the ratio between rapeseed and dye solution was 10 g L^{-1}. All experiments were done under intermittent agitation. Blank solutions were carried out under the same conditions for each test.

The remaining dye concentration was determined by absorption spectrometry (Jasco V-530, Japan UV-VIS spectrophotometer), after sample filtration (by using 0.45 µm filter). Two main parameters characteristic of the sorption process were of interest: sorption removal efficiency and sorption capacity. The dye removal efficiency was determined by the following equation:

$$R\ (\%) = \frac{C_0\text{-}C}{C_0} \cdot 100$$

(1)

where C_0 – initial dye concentration (mg L^{-1}), C – dye concentration after sorption (mg L^{-1}).

The adsorption capacity or the retained amount of dye was calculated with the following equation:

$$q\ \left(mg\ g^{-1}\right) = \frac{C_0\text{-}C}{G} \cdot V$$

(2)

where C_0 and C have the above mentioned meanings, G – weight of rapeseed (g), V – volume of solution (mL).

Influence of initial pH

In order to determine the effect of initial pH of the solution, sorption tests with different values of pH (2-10) were carried out, while the initial concentration of dye was 50 mg L^{-1} (the natural pH of the solution was 5.56). The biomass was allowed to stay in contact with the aqueous phase for 24 h, at room temperature.

Influence of initial dye concentration

In this study, samples of sorbent (0.5 g) were contacted with dye solutions of different concentrations in the range of 25 and 250 mg L^{-1}, at room temperature, under intermittent agitation for 24 h.

Influence of contact time and sorption kinetics

Kinetic measurements consisted in varying the contact time between the solid and aqueous phase. For this, 100 mL solutions with different dye concentrations (50, 100 and 150 mg L^{-1}) were contacted with the appropriate quantity of sorbent, at room temperature and unmodified pH of the solution. The concentration of residual dye was determined at known time intervals: 30, 60, 120 and 240 min. The experimental data was analyzed by the pseudo-first and pseudo-second order kinetic models and the intra-particle diffusion model.

Sorption isotherms

In this study, sorbents were equilibrated with dye solutions of different concentrations (25, 50, 75, 100, 125 and 150 mg L^{-1}) and temperatures (4, 20 and 50 °C). The optimum value of contact time derived from the kinetics study was applied in this section. The initial pH of the solutions was not modified. The most common sorption isotherm models were applied to model the experimental data, namely the Langmuir and Freundlich models, as well as the Dubinin-Radushkevich (D-R) model.

Sorption thermodynamics

The effect of temperature on dye retention on rapeseed was investigated at three different values of temperature: 4, 20 and 50 °C. Thermodynamic parameters, such as Gibbs free energy change (ΔG), enthalpy change (ΔH) and entropy change (ΔS), were determined to evaluate the spontaneity of the process.

RESULTS AND DISCUSSION
Sorbent characterization

Infrared spectroscopy has revealed several functional groups at the surface of rapeseed biomass, which are illustrated in Figure 2. The IR spectra showed a broad band at 3291.94 cm^{-1} characteristic of O-H bond stretching, which is related to the presence of carboxylic and hydroxyl groups found in lignin and cellulose, while the peak at 1036.84 cm^{-1} is assigned to alcoholic groups. The presence of the peak at 2853.96 cm^{-1} is related to aliphatic C-H stretching.[30] The peaks in the region 1742-1651 cm^{-1} mark the stretching of carbonyls of ketones and aldehydes and the region 1500-1000 cm^{-1} is the aromatic region originating from lignin.[42,43]

The surface characteristics and morphology of the biosorbent were observed by the optical microscopy technique. SEM images of rapeseed (Fig. 3a) indicated an uneven and porous structure of the biomass, characterized by heterogeneity. The micrograph of the biomass loaded with RB19 (Fig. 3b) clearly shows the modification of the surface after sorption.
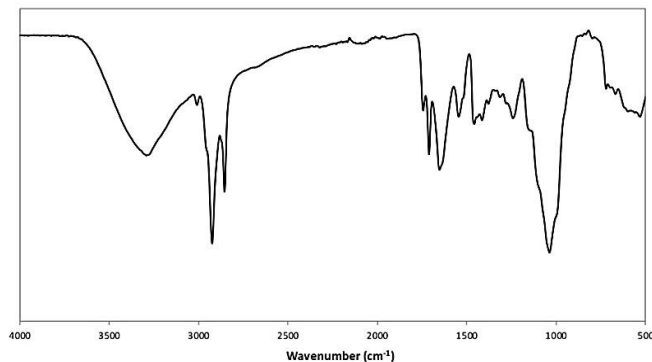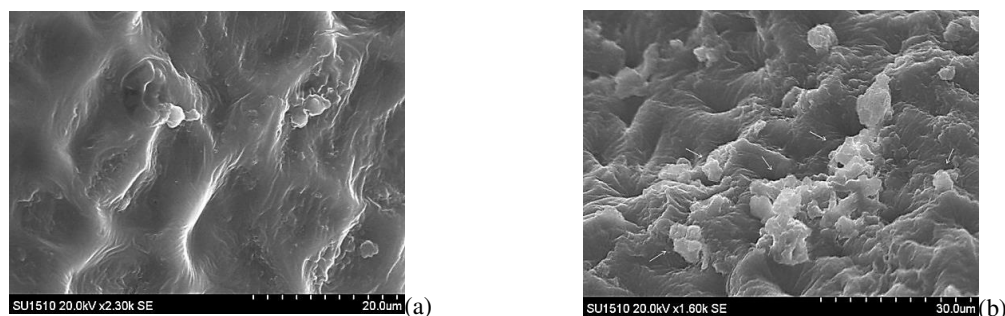
Figure 2: FTIR spectra of rapeseed

Figure 3: SEM images of rapeseed (a) and rapeseed loaded with RB19 (b) (the arrows show the sorption of dye)

Influence of initial pH

The sorption of dyes is dependent on the acidity of the medium, since a variation in the solution pH relates to the modification of superficial charge of the adsorbent, as well as the degree of ionization of the adsorptive molecule.[34]

In the present work, the effect of the sorption behavior of Reactive Blue 19 dye onto rapeseed was determined for pH values of 2, 4, 6 (not adjusted) and 8 for a dye concentration of 50 mg L^{-1} and a ratio of 10 g L^{-1} ($m_{adsorbent}/V_{adsorbate}$), at room temperature. It was observed that there was little change in the equilibrium sorption capacity in the studied pH range. The amount of dye retained from the solution varies slightly, as follows: 5.06 mg g^{-1} (pH $\approx$ 2), 4.97 mg g^{-1} (pH $\approx$ 4), 4.21 mg g^{-1} (pH $\approx$ 6), and 4.57 mg g^{-1} (pH $\approx$ 8). Even though the solution pH is an important factor of influence on the sorption process, it seems that the adsorption of RB19 on rapeseed is independent over the examined pH interval. Similar results were reported for adsorption of reactive orange 16 on chitosan,[44] tropaeolin on castor bean presscake.[45] Data found in the literature indicate an optimum pH range for anionic dye adsorption between 3.0 and 6.0.[46]

Hence, a control on the initial pH was not applied and the tests were conducted at natural pH of the RB19 solutions, which remained around the value of 5.6 after dilution.

The effect of pH on the sorption equilibrium can be explained by various mechanisms. FTIR analysis revealed that the surface of rapeseed contains a number of hydroxyl, carboxyl *etc.* functional groups that can chemically interact with the dye molecule. The pH of the medium influences these interactions by varying the charge on the adsorbate surface.[34,47] Another possible explanation is the existence of electrostatic interactions between the dye molecules and the active sites on the surface of the sorbent. In contrast to the first mechanism, the second mechanism may not be so affected by the pH variation.[48]

The acidity of the medium is also in strong relation with the capacity of dissociation of the dye molecule. At pH values above the isoelectric point, the dissociated form predominates, while at lower values, the molecular form is predominant.[34] In this study, it is most probable that the sorbent prefers any form of the dye molecules.

Influence of initial dye concentration

The effect of initial RB19 dye concentration on sorption behavior is presented in Figure 4. Results indicated a clear increase from 2 to 12.3 mg g^{-1} for a concentration range of 25 to 250 mg L^{-1}. It can be observed that the amount of dye retained on the biomass (q) has a direct relationship with the initial dye concentration. This fact may be reasoned by an increase in the driving force of the concentration gradient with the initial concentration.[42,49] At the same time, the removal efficiency decreases from around 94% to 49% within the same variation of concentration. This can be explained by the saturation or insufficiency of active sites present on the sorbent at higher dye concentrations, meaning that there is a limited number of active and available adsorption sites.[11,47,50] On the other hand, for the same quantity of sorbent, as the initial concentration increases, the remaining amount of dye in the solution increases, leading to a reduction in the removal efficiency.[51]

Sorption kinetics

The rate of sorption is an important parameter is the design of any biosorption system, and it can be determined from the effect of time variation on the sorption process. It is considered that for the sorbate molecule to reach the active centers from the surface of the adsorbent from the solution medium, four transport-resistance stages can exist:[52] (i) the transport of the aqueous phase until the film surrounds the solid particles, (ii) the external diffusion, (iii) the transport within the adsorbent particle, and (iv) the physical or chemical surface reactions.

Figure 5 illustrates the time dependence of the dye uptake by the rapeseed biomass for three different dye concentrations: 50, 100 and 150 mg L^{-1}, respectively. The figure revealed an abrupt increase in the RB19 sorption capacity at the beginning of the tests. Then the sorption rate gradually decreased until the equilibrium was reached in about 240 min. A reason for this phenomenon may be that at longer times, the remaining vacant sites would be more difficult to occupy because of the repulsive forces between the dye molecules on the rapeseed surface and the solution phase.[42,53]

In order to investigate the sorption mechanisms and the rate controlling steps, the kinetics of the process was done by using the pseudo-first-order, pseudo-second-order and intra-particle diffusion models. The pseudo-first-order equation, originally given by Lagergren, is presented in Eq. (3):[52]

$$\lg(q_e - q_t) = \lg(q_e) - \frac{k_1}{2.303}t \tag{3}$$

where q_e (mg g^{-1}) and q_t (mg g^{-1}) are the adsorption capacity at equilibrium and time t (min), respectively, k_1 (min^{-1}) is the Lagergren rate constant. The representation $\lg(q_e$-$q_t)$ vs t gives the values for the constants q_e and k_1, which are presented in Table 1. The coefficients of determination (R^2) varied vastly and the calculated and experimental q_e values were not in agreement. One can conclude that the pseudo-first-order model is not suitable to describe the sorption of RB19 on rapeseed.

The pseudo-second-order used to evaluate the adsorption kinetics may be expressed as follows:[54]

$$\frac{t}{q_t} = \frac{1}{k_2 q_e^2} + \frac{t}{q_e} \tag{4}$$

where k_2 (g mg^{-1} min^{-1}) is the pseudo-second-order rate constant. q_e and k_2 can be deduced from the intercept and the slope of the plot t/q_t against t. According to the data presented in Table 1, the calculated values for q_e were similar to the experimental ones, and high R^2 coefficients ($R^2 > 0.995$) were obtained. These results indicate that the sorption process fits to the pseudo-second-order kinetic model. This model assumes that the dye molecule interacts with two binding sites on the surface of the biosorbent, or that two molecules were adsorbed on a single site.[55]

The experimental data was also fitted to the intra-particle diffusion model,[56] expressed as:

$$q_t = k_{id} t^{0.5} \tag{5}$$

where k_{id} (mg g^{-1} min$^{-0.5}$) is the intra-particle diffusion rate, C (mg g^{-1}) is related to the thickness of the boundary layer. The model's constants were calculated from the plot q_t vs $t^{0.5}$. As shown in Table 1, R^2 was fairly low (≤ 0.9) and hence, it does not describe very well the sorption of RB19. A similar result was obtained for biosorption of Acid Blue 25 dye on shrimp shell.[57] These results indicate that diffusion is not the rate-limiting step in the RB19 sorption on rapeseed.
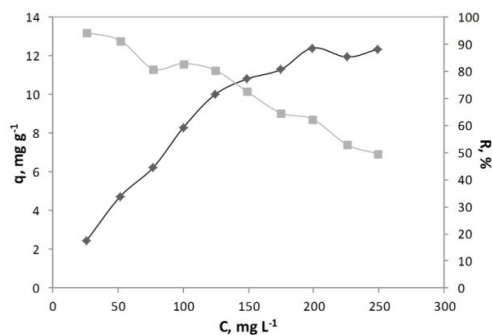
Figure 4: Effect of initial dye concentration on biosorption of RB19 on rapeseed, q, mg g^{-1} (♦), R, % (■)
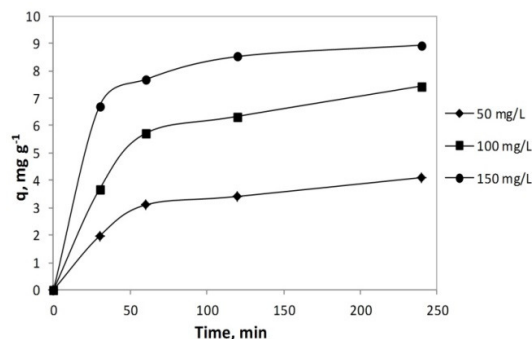

Figure 5: Effect of contact time for the sorption of RB19 onto rapeseed biomass (10 g L^{-1} sorbent, 20 °C)

Table 1
Kinetic parameters by pseudo-first order, pseudo-second order, intra-particle and film diffusion models for RB19 dye biosorption on rapeseed at different initial dye concentrations; sorbent dose = 10 g L^{-1}, T = 20 °C

C_0 (mg g^{-1})	Pseudo-first order model			Pseudo-second order model			Intra-particle diffusion model		Film diffusion model		
	k_1 10^{-3} (min^{-1})	q_e (mg g^{-1})	R^2	k_2 10^{-3} (mg g^{-1} min^{-1})	q_e (mg g^{-1})	R^2	k_{id} (mg g^{-1} min$^{-0.5}$)	R^2	k_f (min^{-1})	b	R^2
50	6.7	2.85	0.951	5.3	4.75	0.995	0.19	0.889	0.0067	0.49	0.951
100	6.4	5.00	0.942	3.2	8.55	0.996	0.34	0.880	0.0063	0.54	0.942
150	4.6	6.54	0.967	3.1	10.58	0.995	0.37	0.949	0.0046	0.58	0.967

The film diffusion model is expressed with the following equation:[40,58]

$$\ln\left(1 - \frac{q_t}{q_e}\right) = -k_f t - b$$

(6)

where k_f (min^{-1}) is the film diffusion rate constant, b is the model's constant. The value of k_f can be calculated from the plot $\ln(1-q_t/q_e)$ versus t. The results are presented in Table 1. From the values of b constant, it can be observed that the linear plots do not pass through the origin and thus, film diffusion is not the only rate-limiting step. It can be concluded that both intra-particle diffusion and film diffusion contribute to the kinetic rate of the process.

Sorption isotherm studies

Equilibrium studies are paramount for understanding the mechanism of sorption. The sorption isotherms give information about the interaction of dye molecules with adsorbent active sites during the adsorption process.[59] Various isotherm models, like Langmuir, Freundlich and Dubinin-Raduskevich, were applied to fit the equilibrium data for the sorption of RB19 on the rapeseed.

Langmuir adsorption isotherm is one of the most common empirical models used, which assumes a monolayer uptake of the adsorbate involving specific and finite number of homogenous sites within the adsorbent.[11]

The Langmuir mathematical relationship in linear form can be expressed as follows:[60,61]

$$\frac{1}{q_e} = \frac{1}{q_m} + \frac{1}{q_m K_L C_e}$$

(7)

where q_e (mg g^{-1}) is the dye uptake per unit mass of rapeseed at equilibrium, q_m (mg g^{-1}) is the maximum sorption capacity, K_L is the Langmuir constant (related to the affinity between the adsorbate and adsorbent) and C_e (mg L^{-1}) is the equilibrium dye concentration in solution. The values of q_m and K_L can be determined from the intercept and the slope, respectively, of the linear plot $1/q_e$ *versus* $1/C_e$ (Fig. 6a). The values for Langmuir parameters are listed in Table 2. The goodness of the experimental data fit was measured by the coefficient of determination, R^2. In the case of this study, the R^2 values obtained were 0.9866, 0.9880 and 0.9942 at temperatures of 4, 20 and 50 °C, respectively.
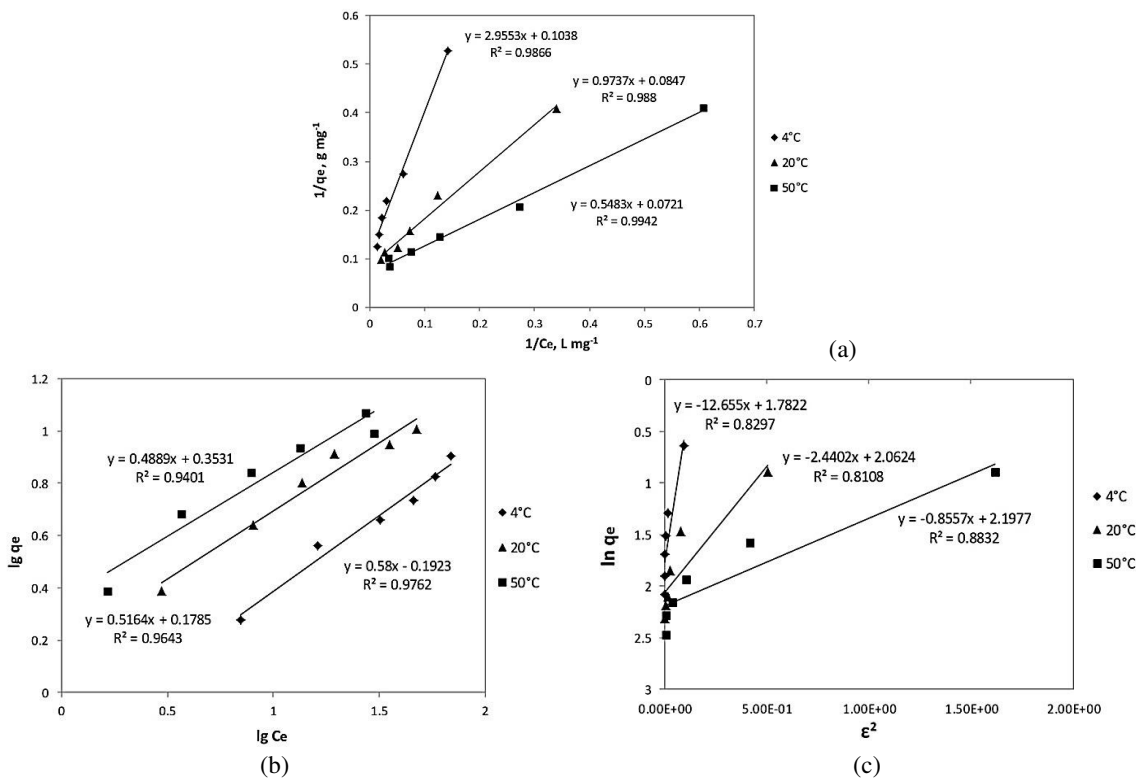
Figure 6: Isotherm plots for the sorption of RB19 dye onto rapeseed (10 g L^{-1} rapeseed, 240 min): (a) Langmuir, (b) Freundlich, (c) Dubinin-Raduskevich

Table 2
Sorption isotherm parameters used for RB19 dye biosorption by rapeseed at different temperatures; rapeseed dose 10 g L^{-1}

Isotherm model	Parameters	Values		
		4°C	20°C	50°C
Langmuir	q_m, mg g^{-1}	9.63	11.81	13.86
	K_L x 10^{-2}, L mg^{-1}	3.51	8.69	13.15
	R_L	0.16 – 0.52	0.07 – 0.29	0.05 – 0.22
Freundlich	n	1.72	1.94	2.05
	K_F	1.56	1.51	2.25
Dubinin-Raduskevich	$-\beta$, mol^2 J^{-2}	12.65	2.44	0.85
	q_s, mg g^{-1}	5.94	7.86	9.00
	E, J	0.20	0.45	0.77

The verification of the Langmuir isotherm confirms the homogenous nature of the adsorption in a single layer of RB19 dye onto rapeseed at each of the mentioned temperature values.

The Langmuir constant can be used to indicate the favorability of the adsorption process by using a dimensionless separation factor, R_L:

$$R_L = \frac{1}{1 + K_L C_0}$$

(8)

where C_0 (mg g^{-1}) is the initial dye concentration.

Depending on the value obtained for this parameter, the adsorption can be: unfavorable ($R_L > 1$), linear ($R_L = 1$), favorable ($0 < R_L < 1$) or irreversible ($R_L = 0$).[51] At all temperatures, the calculated values for R_L (Table 2) were below unit, suggesting a favorable retention of the organic molecules on the rapeseed surface.

The Freundlich isotherm model assumes the existence of heterogeneity among the active sites and non-uniform heat distribution, and has been used for multilayer adsorption systems.[62]

The following Freundlich isotherm equation was applied:[63]

$$\lg q_e = \lg K_F + \frac{1}{n}\lg C_e$$

(9)

where q_e (mg g^{-1}) is the amount of dye adsorbed at equilibrium, C_e (mg L^{-1}) is the equilibrium concentration of the sorbate, K_F and n are the Freundlich constants.

The plot of $\lg q_e$ against $\lg C_e$ is presented in Figure 6b. The experimental data fitted fairly well the Freundlich model, giving linear curves with coefficients of determination higher than 0.94. Nevertheless, the R^2 values were lower than the ones for the Langmuir isotherm. The model's constants can be calculated from the intercept and slope, respectively and can be found listed in Table 2. Values above the unit for all temperatures in the case of parameter n indicate favorable adsorption.

The Dubinin-Raduskevich (D-R) isotherm model has been employed for the evaluation of the characteristic porosity of the sorbent and the apparent free energy of adsorption. The equation to describe the interaction between the adsorbate and adsorbent at equilibrium in this case can be expressed as follows:[42]

$$\ln q_e = \ln q_s - \beta\varepsilon^2$$

(10)

where q_e (mg g^{-1}) is the amount of dye retained on the solid at equilibrium, q_s (mg g^{-1}) is the theoretical saturation capacity, β (mol^2 J^{-2}) is activity coefficient and ε (J^2 mol^{-2}) is the Polanyi potential, which is a function of the equilibrium concentration (C_e, mg g^{-1}).

$$\varepsilon = RT\ln\left(1+\frac{1}{C_e}\right)$$

(11)

where R is the universal gas constant (8.31 J mol^{-1} K^{-1}) and T is the temperature (K).

The plot $\ln q_e$ *versus* ε^2, depicted in Figure 6c, is of help for determining the activity coefficient β and adsorption capacity at the studied temperatures, listed in Table 2. The affinity coefficient is related to the sorption energy, E (kJ):

$$E = \frac{1}{\sqrt{-2\beta}}$$

(12)

The mean sorption energy, *E*, can give information about the type of mechanism involved: if $E < 8$ kJ mol^{-1}, the biosorption process can be considered to be controlled by a physical mechanism; if $8 < E < 16$ kJ mol^{-1}, an ion-exchange mechanism is involved, and if $E > 16$ kJ mol^{-1}, the sorption takes place by a chemical reaction.[45]

The D-R isotherm model has shown a lower applicability than the other used models in the RB19 dye sorption on rapeseed ($R^2 < 0.88$). Nevertheless, a mean energy lower than 8 kJ mol^{-1} indicates that the biosorption mechanism was likely to be a physical phenomenon. Similar results were obtained by Fathi *et al.*[6] when studying the adsorption of Direct Red 23 on corn stalks.

Sorption thermodynamics

The study of thermodynamic parameters was done in order to evaluate the feasibility and nature of the sorption process. The following equations were used to determine various thermodynamic parameters, such as variation in standard Gibbs free energy (ΔG^0), variation in enthalpy (ΔH^0) and variation in entropy (ΔS^0):[34,37]

$$\Delta G^0 = -RT\ln K_c$$

(13)

$$K_c = \frac{C_a}{C_e}$$

(14)

$$\ln K_C = \frac{\Delta S}{R} - \frac{\Delta H}{RT}$$

(15)

where R is the ideal gas constant (0.0083 kJ mol^{-1} K^{-1}), T (K) is temperature, K_c is the equilibrium constant, expressed as the ratio of adsorbed dye concentration, C_a (mg g^{-1}), and the residual dye concentration in the solution, C_e, (mg g^{-1}). The constant K_c has been calculated from the representation of C_a/C_e vs C_a, as the intercept of the linear plot for each temperature (Table 3). Then these values were used in the plot $\ln K_C$ vs $1/T$ to obtain the parameters ΔH and ΔS (Fig. 7). The results are shown in Table 3. The negative values for the Gibbs free energy changes and the positive value in the enthalpy change indicate the spontaneous and endothermic nature of the process. It was observed that the amount of adsorbed dye improves with the increase of solution temperature (Table 2), which also proves that the process exhibits an endothermic nature. An increase in the temperature might enhance the mobility of the dye molecules,[11] while facilitating the access to the active centers of the sorbent due to an increase in the free volume.[40,42] The positive value of ΔH and the increase of energy activation at elevated temperatures, as presented in Table 2, indicate the existence of an energy barrier in the dye uptake by rapeseed.[34]

The process is spontaneous ($\Delta S > 0$), meaning the randomness at the solid-liquid interface has increased due to adsorption.[37]
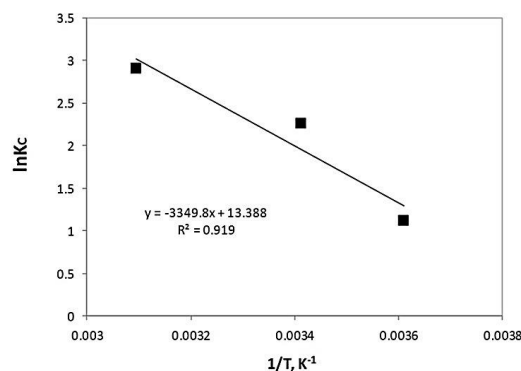

Figure 7: Plot of thermodynamic equilibrium constant (ln K_C) against temperature ($1/T$) for thermodynamic parameters determination

Table 3
Thermodynamic parameters of dye biosorption on rapeseed at different temperatures

T (°C)	K_C	ln K_C	ΔG (kJ mol^{-1})	ΔH (kJ mol^{-1})	ΔS (kJ mol^{-1} K^{-1})
4	3.04	1.11	-2.56		
20	9.49	2.25	-5.47	27.80	0.11
50	18.25	2.90	-7.78		

CONCLUSION

The removal of Reactive Dye 19 from aqueous solution by sorption onto rapeseed was investigated under different operational conditions. The FTIR spectra and SEM micrographs confirmed the biosorption of dye on rapeseed. The amount of RB19 that was undertaken by rapeseed through sorption was found to vary with solution pH, initial dye concentration, contact time and temperature. The kinetic modeling was done by using several mathematical models, such as the pseudo-first and pseudo-second kinetic models, as well as the intra-particle and film diffusion models. It was found that biosorption is a complex process and the sorption rate is highly dependent on the intrinsic surface reaction, intra-particle diffusion and film mass transfer. The empirical equations used to describe the sorption equilibrium showed that the process was reversible and followed the physical sorption mechanism. The Langmuir model gave the highest fit ($R^2 > 0.98$), indicating a single layer coverage of the rapeseed surface. The maximum sorption capacity obtained was 11.81 mg g^{-1} at room temperature. Thermodynamic parameters (ΔG, ΔH and ΔS) were calculated. The results indicated the endothermic and spontaneous nature of the process. The positive value of ΔS denotes that adsorption is based on the electrostatic interaction between the dye molecule and biomass.

Removal efficiencies of up to 94.26% were reported for this study, thus proving the possibility to use rapeseed in the sorptive treatment of aqueous solutions containing Reactive Blue 19.

REFERENCES
[1] A. Mittal, J. Mittal, A. Malviya, D. Kaur and V. K. Gupta, *J. Colloid. Interf. Sci.*, **343**, 463 (2010).
[2] A. Ozcan, C. Omeroglu, Y. Erdogan and A. S. Ozcan, *J. Hazard. Mater.*, **140**, 173 (2007).
[3] F. Ferrero and M. Periolatto, *Clean Tech. Environ. Policy*, **14**, 487 (2012).
[4] M. Siddique, R. Farooq, A. Khalid, A. Farooq, Q. Mahmood *et al.*, *J. Hazard. Mater.*, **172**, 1007 (2009).
[5] C. R. Holkar, A. B. Pandit and D. V. Pinjari, *Bioresour. Technol.*, **173**, 342 (2014).
[6] N. A. Fathy, S. E. El-Shafey, O. I. El-Shafey and W. S. Mohamed, *J. Environ. Chem. Eng.*, **1**, 858 (2013).
[7] E. Alventosa-deLara, S. Barredo-Damas, M. I. Alcaina-Miranda and M. I. Iborra-Clar, *J. Hazard. Mater.*, **209-210**, 492 (2012).
[8] Y. Zheng, G. Yao, Q. Cheng, S. Yu, M. Liu *et al.*, *Desalination*, **328**, 42 (2013).

9   N. M. Mahmoodi, R. Salehi and M. Arami, *Desalination*, **272**,187 (2011).

10   M. Asgher, *Water Air Soil Pollut.*, **223**, 2417 (2012).

11   M. T. Yagub, T. K. Sen, S. Afroze and H. M. Ang, *Adv. Colloid Interface Sci.*, **209**, 172 (2014).

12   H. Ali, *Water Air Soil Pollut.*, **213**, 251 (2010).

13   B. Bonakdarpour, I. Vyrides and D. C. Stuckey, *Int. Biodeter. Biodegr.*, **65**, 591 (2011).

14   D. Cui, G. Li, D. Zhao, X. Gu, C. Wang *et al.*, *J. Hazard. Mater.*, **221-222**, 185 (2012).

15   J. M. Fanchiang and D. H. Tseng, *Chemosphere*, **77**, 214 (2009).

16   S. Wang, *Dyes Pigments*, **76**, 714 (2008).

17   J. M. Poyatos, M. M. Munio, M. C. Almecija, J. C. Torres, E. Hontoria *et al.*, *Water Air Soil Pollut.*, **205**, 187 (2010).

18   D. Cailean, G. Barjoveanu, C. P. Musteret, N. Sulitanu, L. R. Manea *et al.*, *Environ. Eng. Manag. J.*, **8**, 503 (2009).

19   M. Siddique, R. Farooq, Z. M. Khan, Z. Khan and S. F. Shaukat, *Ultrason. Sonochem.*, **18**, 190 (2011).

20   J. O. Tijani, O. O. Fatoba, G. Madzivire and L. F. Petrik, *Water Air Soil Pollut.*, **225**, 2102 (2014).

21   M. A. N. Khan, M. Siddique, F. Wahid and R. Khan, *Ultrason. Sonochem.*, **26**, 370 (2015).

22   A. Duta and M. Visa, *J. Photoch. Photobio. A*, **306**, 21 (2015).

23   A. Hebeish, M. A. Ramadan, E. Abdel-Halim and A. Abo-Okeil, *Clean Tech. Environ. Policy*, **13**, 713 (2011).

24   M. Visa, F. Pricop and A. Duta, *Clean Tech. Environ. Policy*, **13**, 855 (2011).

25   L. D. Fiorentin, D. E. G. Trigueros, A. N. Modenes, F. R. Espinoza-Quinones, N. C. Pereira *et al.*, *Chem. Eng. J.*, **163**, 68 (2010).

26   S. Rangabhashiyam, N. Anu and N. Selvaraju, *J. Environ. Chem. Eng.*, **1**, 629 (2013).

27   T. Akar, S. Turkyilmaz, S. Celik and S. T. Akar, *J. Clean. Prod.*, **112**, 4844 (2015).

28   V. S. Tran, H. H. Ngo, W. Guo, J. Zhang, S. Liang *et al.*, *Bioresour. Technol.*, **182**, 353 (2015).

29   A. Abdolali, W. S. Guo, H. H. Ngo, S. S. Chen, N. C. Nguyen *et al.*, *Bioresour. Technol.*, **160**, 57 (2014).

30   A. Ebrahimian, E. Saberikhah, M. S. Emami and M. Sotudeh, *Cellulose Chem. Technol.*, **48**, 735 (2014).

31   M. Perez-Ameneiro, G. Bustos, X. Vecino, L. Barbarosa-Pereira, J. M. Cruz *et al.*, *Water Air Soil Pollut.*, **226**, 133 (2015).

32   A. Bhatnagar, M. Sillanpaa and A. Witek-Krowiak, *Chem. Eng. J.*, **270**, 244 (2015).

33   Z. M. Magriotis, S. S. Vieira, A. A. Saczk, N. A. V. Santos and N. R. Stradiotto, *J. Environ. Chem. Eng.*, **2**, 2199 (2014).

34   N. M. Mahmoodi, M. Arami, H. Bahrami and S. Khorramfar, *Desalination*, **264**, 134 (2010).

35   A. Mittal, D. Kaur and J. Mittal, *J. Colloid. Interf. Sci.*, **126**, 8 (2008).

36   C. G. Rocha, D. A. M. Zaia, R. V. S. Alfaya and A. A. S. Alfaya, *J. Hazard. Mater.*, **166**, 383 (2009).

37   M. E. Argun, D. Guclu and M. Karatas, *J. Ind. Eng. Chem.*, **20**, 1079 (2014).

38   M. Asgher and H. N. Bhatti, *Can. J. Chem. Eng.*, **90**, 412 (2012).

39   S. Sadal, H. N. Bhatti, S. Nausheen and M. Amin, *J. Taiwan Inst. Chem. E.*, **47**, 160 (2015).

40   S. Karmaker, N. M. Uddin, H. Ichikawa and Y. Fukumori, *J. Environ. Chem. Eng.*, **3**, 583 (2015).

41   D. Suteu, T. Malutan and D. Bilba, *Cellulose Chem. Technol.*, **45**, 413 (2011).

42   M. R. Fathi, A. Asfaram and A. Farhangi, *Spectrochim. Acta A*, **135**, 364 (2015).

43   L. M. Kline, D. G. Hayes, A. R. Womac and N. Labbe, *BioResources*, **5**, 1366 (2010).

44   S. Rosa, M. C. M. Laranjeira, H. G. Riela and V. T. Favere, *J. Hazard. Mater.*, **155**, 253 (2008).

45   Z. M. Magriotis, S. S. Vieira, A. A. Saczk, N. A. V. Santos and N. R. Stradiotto, *J. Environ. Chem. Eng.*, **2**, 1731 (2014).

46   D. Asandei, V. Dulman, T. Todorciuc and E. Bobu, *Cellulose Chem. Technol.*, **47**, 799 (2013).

47   C. Paduraru, L. Tofan, C. Teodosiu, I. Bunia, N. Tudorachi *et al.*, *Process Saf. Environ.*, **94**, 18 (2015).

48   A. Sharma and K. G. Bhattacharyya, *J. Hazard. Mater.*, **125**, 102 (2005).

49   G. Z. Kyzas, P. I. Siafaka, E. G. Pavlidou, K. J. Chrissafis and D. N. Bikiaris, *Chem. Eng. J.*, **259**, 438 (2015).

50   T. Todorciuc, L. Bulgariu and V. I. Popa, *Cellulose Chem. Technol.*, **49**, 439 (2015).

51   M. Malakootian, H. J. Mansoorian, A. Hosseini and N. Khanjani, *Process Saf. Environ.*, **96**, 125 (2015).

52   K. D. Belaid, S. Kacha, M. Kameche and Z. Derriche, *J. Environ. Chem. Eng.*, **1**, 496 (2013).

53   M. Kousha, E. Daneshvar, S. M. Sohrabi, M. Jokar and A. Bhatnagar, *Chem. Eng. J.*, **192**, 67 (2012).

54   Y. S. Ho and G. McKay, *Process Biochem.*, **34**, 451 (1999).

55   F. Hemmati, R. Norouzbeigi, F. Sarbisheh and H. Shayesteh, *J. Taiwan Inst. Chem. E.*, **58**, 482 (2016).

56   W. J. Weber and J. C. Morris, *J. Sanit. Eng. Div. Am. Soc. Civ. Eng.*, **89**, 31 (1963).

57   E. Daneshvar, M. S. Sohrabi, M. Kousha, A. Bhatnagar, B. Aliakbarian *et al.*, *J. Taiwan Inst. Chem. E.*, **45**, 2926 (2014).

58   C. Yao and T. Chen, *Chem. Eng.*, **265**, 93 (2015).

59   U. A. Isah, G. Abdulraheem, S. Bala and S. Muhammad, *Int. Biodeter. Biodegr.*, **102**, 265 (2015).

60   I. Langmuir, *J. Am. Chem. Soc.*, **38**, 2221 (1916).

61   K. Y. Foo and B. H. Hameed, *Chem. Eng. J.*, **156**, 2 (2010).

62   S. Rangahashiyam, N. Anu, M. S. G. Nandagopal and N. Selvaraju, *J. Environ. Chem. Eng.*, **2**, 398 (2014).

63   H. Freundlich, *J. Phys. Chem.*, **57**, 385 (1906).